

Performance, Combustion and Emission analysis of pongamia oil of Biodiesel engine with an nano additives: an Experimental Study

Kumara B¹, C R Raghavendra²,

^aDepartment of Mechanical Engineering, ACS College of Engineering, Bangalore, Karnataka, India
Visvesvaraya Technological University, Belagavi, Karnataka- 560098

^bDepartment of Mechanical Engineering, Government Engineering College, Haveri, Karnataka, India
Visvesvaraya Technological University, Belagavi, Karnataka- 560098

DOI: <https://doie.org/10.0618/Jbse.2024674025>

ABSTRACT

The urgent need to find alternative fuel sources for internal combustion engines arises from the swift exhaustion of crude oil reserves and the resulting environmental harm. Biodiesel emerges as a hopeful contender for compression ignition Biodiesel engines owing to its favorable heat content and combustion characteristics. Employed in a wide range of vehicles and machinery including cars, trucks, buses, off-road vehicles, and oil furnaces, Biodiesel blends offer significant emissions reduction potential of up to 77% from Biodiesel engines while also enhancing engine longevity due to their superior lubricating properties. However, biodiesel presents certain limitations, such as diminished performance and heightened nitrogen oxide emissions. As a result, the focus of this research is to explore the utilization of locally accessible biodiesel in a low-heat rejection engine, supplemented with nano additives, with the objective of enhancing performance while mitigating nitrogen oxide emissions. India presently boasts numerous biodiesel sources, encompassing vegetable oil and pongamia oil, which can be efficiently harnessed in Biodiesel engines through the incorporation of fatty acid ester and glycerol. The valid experimental setup comprises a single-cylinder 4-stroke water-cooled Biodiesel engine generating 5.2 kW of power. A water-cooled piezoelectric pickup, with a range from 0 to 250 bar, was installed on the cylinder head to measure engine cylinder pressure. Crankshaft position was determined using an optical crank angle (CA) encoder (Manufacturer: Kistler, Model: Type 2613B) to measure cylinder pressure at various crank angles. Both coated and uncoated engines underwent testing with varying proportions of pongamia oil. The key findings demonstrate a significant enhancement in engine performance across all loads compared to the baseline engine. Furthermore, when combined with L-ascorbic acid, these Biodiesels exhibit a notable reduction in nitrogen oxide emissions.

Keywords: Bioiesel Engine, pongamia oil, nitrogen oxide emissions

1. Introduction

The experimental configuration features a single-cylinder 4-stroke water-cooled Biodiesel engine producing 5.2 kW of power. To monitor engine cylinder pressure, a water-cooled piezoelectric pickup with a range from 0 to 250 bar was affixed to the cylinder head. Crankshaft position was tracked utilizing an optical crank angle (CA) encoder (Manufacturer: Kistler, Model: Type 2613B) to measure cylinder pressure at different crank angles. Tests were conducted on both coated and uncoated engines using different blends of pongamia oil. The final results reveal a considerable improvement in engine performance under all operating conditions compared to the standard engine proper configuration. Moreover, the incorporation of L-ascorbic acid with these biodiesels leads to a substantial decrease in nitrogen oxide emissions.

Esterification/transesterification techniques were employed in the production process. The necessity for multiple processing stages represents more than 70% of the overall production expenditure of biodiesel when refined oil is utilized as the feedstock. Accordingly, the adoption of a combined process involving extraction, esterification, and transesterification, also referred to as reactive extraction, holds promise for reducing processing expenses. Reactive-extraction deviates from the traditional biodiesel production selected method wherein the oil-bearing material interacts directly with alcohol instead of reacting with pre-extracted oil. Essentially, extraction and transesterification occur simultaneously, with alcohol serving as both an extraction solvent and a transesterification reagent. Since its inception by Harrington and D'arcy Evans, various researchers have scrutinized the efficacy and viability of this approach. Yet, the potential for replacing the existing transesterification technology with reactive-extraction remains uncertain. The realization of biodiesel production through reactive-extraction hinges on the comprehensive characterization of the entire used process. Multiple parameters influence the process of reactive extraction of oil-bearing biomass for biodiesel production. Additionally, Haas et al. highlighted that biodiesel generated through reactive-extraction tends to incur higher costs compared to biodiesel produced via conventional transesterification, mainly due to the substantial methanol quantities necessary for the process. The implementation of reactive-extraction not only streamlines the process but also eliminates the necessity for a dedicated step to extract hazardous substances during downstream processing, thereby decreasing workers' exposure to such compounds. This methodology, however, can be applied to nearly any lipid-bearing material. Several studies document the utilization of an incubator shaker in biochemical and biocatalytic reactions. The esterification reactions involving 4-methyloctanoic acid (4-MOA) with PEG in an organic monophasic and water/organic biphasic system, utilizing Novozym435 R as the catalyst, were conducted in a New Brunswick Scientific Innova TM 4080 incubator shaker operating at 350 rpm and 45°C. Likewise, enzymatic transesterification was conducted to convert racemic 4-methyl hexanoic acid methyl ester and 4-methyloctanoic methyl ester into their respective butyl esters, utilizing a New Brunswick Scientific Innova TM 4080 incubator shaker. Furthermore, important studies have explored the extraction of algae oil and its subsequent transesterification, performed in an electric shaker at 300 rpm for 3 hours. The current investigation focuses on evaluating the impact of various important parameters on the reactive extraction of Pongamia seeds for biodiesel production, utilizing an incubator shaker in the author's research laboratory as shown in figure.



Figure 1: Four stroke diesel engine setup in Lab

The study aims to collect biodiesel from pongamia and Jatropha oil through the process of transesterification. Following this, blending conventional diesel with pongamia and Jatropha biodiesel, along with nano additives, is carried out to create a blend known as B40. Optimization of engine operating conditions, encompassing load, compression ratio, and injection pressure, is pursued to maximize performance parameters and minimize emission levels when utilizing different proportions of biodiesel and its additives. Experimental analysis on the B40 blend, along with different nano additives such as Al₂O₃, SiO₂, and TiO₂, is conducted at varying loads and injection pressures. Additionally, the influence of injection pressure of the B40 blend diesel, along with nano additives, and different loads applied on the engines is investigated. The study also delves into the performance and characteristics of engines using B40 biodiesel with nano additives, focusing on combustion, emissions, and performance, including brake thermal efficiency and specific fuel combustion. Furthermore, exhaust gas temperature and smoke analysis emission tests are conducted for NO_x and CO_x analysis.

2. Experimental Methodologies

The present work involves the setting up of transesterification process set up and experimental test rig of CI engine. Therefore, an experimental set up was made with necessary instrumentation in order to evaluate the performance, emission and combustion parameters of the compression ignition engine at different operating conditions. Crude vegetable oils have higher viscosity and are undesirable. It is therefore necessary to reduce the viscosity and separate the glycerin content of vegetable oil. For this purpose, the transesterification of vegetable oil is more suitable for all vegetable oils. This chapter discusses the details of the transesterification setup, experimental setup, instruments used and development of certain components and software needed for the work.

2.2. Pongamia

Millettia pinnata, also referred to as *P. pinnata*, is an evergreen tree prevalent in the rainforests of Asia, specifically in the region of Pongamia. The tree typically begins yielding pods around the fifth year of growth, with pod production increasing gradually until stabilizing around the twelfth year. Pongamia oil, extracted from the seeds, can be obtained through mechanical expeller, cold pressing, or solvent extraction techniques, resulting in an oil with a yellowish-orange to brown hue.



Figure 2: Pongamia pod and seed.

3.1 Transesterification

The transesterification set up consists of a 2 liter capacity round bottom flask with three necks to it and is placed in a water container for heating the oil [Fig. 1]. A heater with temperature regulator was used for heating the oil in the round bottom flask. A high speed motor with a magnetic stirrer in the form of rotating element was used for mixing the oil vigorously. In the transesterification process triglycerides of Honge oil react with methyl alcohol in the presence of a catalyst (NaOH/KOH) to produce fatty acid ester and glycerol. In this process 1000 gm of Honge oil, 240 gm methanol and 8 gm sodium hydroxide were taken in a round bottom flask. Fig. 2 show items required for transesterification process such as Methanol, Sodium hydroxide, Sodium Sulfate and Silica gel containers. All the contents were heated up to 70⁰C and stirred by the magnetic stirrer vigorously for one hour when the ester formation begins. The mixture was transferred to a separating funnel and allowed to settle down under gravity for overnight. The upper layer in the separating funnel forms the ester and the lower layer being glycerol was removed from the mixture [Fig.3]. The separated ester was mixed with 250 gm of hot water and allowed to settle under gravity for 24 hours. Water washing removes the fatty acids and catalyst dissolved in the lower layer and was separated. Fatty acids and dissolved catalyst were removed by using a separator funnel. Silica gel crystals were added to remove the moisture from the ester [Fig. 4].



Figure 3: Equipment for Transesterification



Figure 4: Methanol, Sodium hydroxide, Sodium Sulfate and Silica gel containers



Figure 5: Separation of HOME and Glycerin



Figure 6: Washing and moisture removal from HOME

3.2 Properties of Test Fuels (after Transesterification)

Figure 7 illustrates the flow diagram for biodiesel production, while Table 1 presents the physical properties of diesel, nano additives such as TIO₂, SIO₂, and AL₂O₃ (100%), and pongamia methyl ester (100%). These fuel properties are assessed using ASTM D 6751, which is a prescribed method for testing fuel properties. The density of pongamia oil with nano additives such as TIO₂, SIO₂, and AL₂O₃ exceeds the EN14214 limit of 0.86–0.9, whereas the densities of other biodiesels fall within the prescribed limits and closely resemble that of diesel. Additionally, the kinematic viscosity of nano additives such as TIO₂, SIO₂, and AL₂O₃ is lower compared to other biodiesels and is much closer to that of Biodiesel. The cetane numbers of all biodiesels surpass those of diesel, indicating a higher self-ignition temperature. Table 1 displays the properties of Biodiesel, TIO₂ (20%), SIO₂m AL₂O₃ (20%), and pongamia oil (20%). The investigation of both 20% and 100% biodiesel blends in this study can be attributed to several factors.

The practicality of these blends is a primary consideration. A 20% biodiesel blend, known as B20, enjoys widespread use in various regions and is readily accessible in the market. Its extensive testing has demonstrated effective performance in existing diesel engines, often without the need for significant modifications. Through studying the performance and emission characteristics of B20, researchers can glean valuable insights into its practical application and assess its potential as a viable alternative fuel. Additionally, regulatory requirements may influence the choice of these specific blends. In certain countries or regions, regulations or standards may require the utilization of a minimum biodiesel blend, such as B20, for certain applications or to achieve specific emission reduction targets. Thus, conducting investigations on B20 enables researchers to evaluate compliance with these regulations and comprehend the effects of such blends on engine performance and emissions. Conversely, studying the use of 100% biodiesel (B40) is essential for fully exploring biodiesel's potential as a standalone fuel.

This facilitates researchers in evaluating the performance and emission characteristics exclusively with biodiesel, devoid of any petroleum-based diesel fuel. Gaining insights into the behavior of B40 elucidates the utmost potential of biodiesel as a sustainable and renewable fuel source for diesel engines. Encompassing a spectrum of biodiesel concentrations, ranging from 20% to 100% blends, this investigation enables a comprehensive assessment of their impact on engine performance, emissions, and compliance with regulatory standards.

Table 1: Properties of fuels used

Properties	Diesel	pongamia	HOME	B20	B40	B40Al2O380	B40SiO280	B40TiO2
Chemical Formula	C ₁₃ H ₂₄	----	----	----	----	----	-	-
Density (kg/m ³)	840	927	890	835	856	880	875	862
Calorific value (kJ/kg)	43,000	35,800	36,010	41,856	41,296	41,476	41,368	41,558
Viscosity (cSt)	2-5	56	5.6	4.12	4.46	4.84	4.7	4.6
Flashpoint (°C)	75	187	163	104	108	120	124	130
Cetane Number	45-55	40	45	----	----	----
Carbon Residue (%)	0.1	0.66	----	----	----	----

4. Experimental Setup

Load testing was conducted utilizing a single-cylinder CI engine connected to an eddy current dynamometer for load variation. Load measurement was facilitated by a load cell affixed to the dynamometer arm. The setup allows for measurement of both fuel flow rate and air flow rate into the engine, along with provisions for measuring and regulating the coolant flow rate. Crank angle encoder technology was employed to gauge piston position, while a PCB piezo electronics pressure transducer was utilized to measure in-cylinder gas pressure.

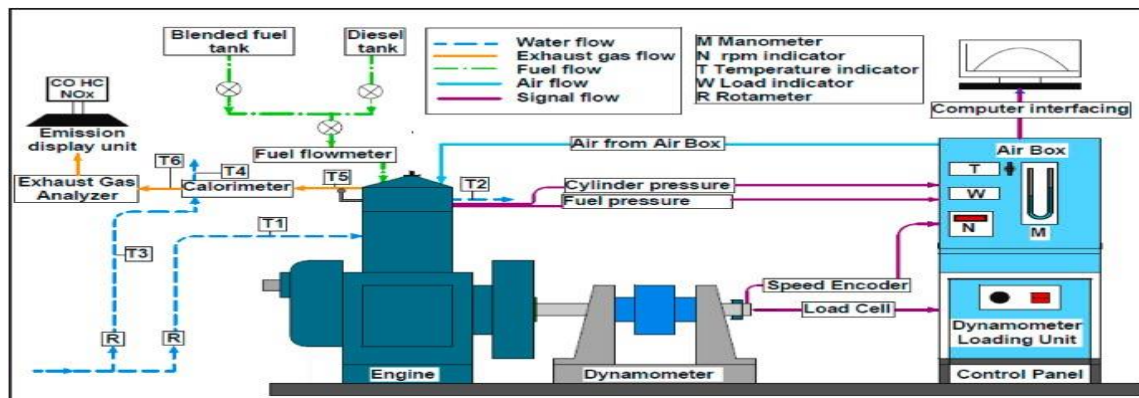


Figure 7: Photographic view of the experimental setup.

The AVL 444 digas analyzer and AVL smoke meter are utilized to measure the engine exhaust emissions. The experimental setup, complete with the necessary equipment, is depicted in Figure 7. The engine is capable of operating with neat diesel at a consistent speed of 1500 rpm to achieve a steady-state condition. Both the exhaust gas analyzer and smoke meter are activated well in advance to allow for the stabilization of all systems before the commencement of the experiment.

The above experimental procedure is followed for conducting all experiments. The details of the experiments for the present investigation are as follows:

1. After completing the experiments with neat diesel, the same experimental procedure is repeated with a B20 blend of the pongamia oil with three nano additives such as TIO₂, SIO₂, and AL₂O₃. The experiments and similar observations are repeated with the B40 for TIO₂, SIO₂, and AL₂O₃. After completing the experiment with the said additives Biodiesel, the engine is allowed to run for about half an hour with Biodiesel to eliminate interference from the previous Biodiesel fuel.
2. The experiments for nano additives and pongamia oil for 20 and 100% proportions are conducted similarly.
3. The experiment for B20 and B40 of nano additives and pongamia oil in a lanthanum oxide- is conducted.
4. Different proportions of LA were added with Biodiesel, and experiments were conducted in a conventional engine to find the optimum proportion of LA.
5. Experiments are conducted with different proportions of LA with B20 and B40 of three Biodiesel blends in conventional engines.

5. Results and Discussion

5.1. Diesel blends with pongamia oil and nano additives

Biodiesels and pongamia oil with nano additives by 20 and 100% proportions. The experiments for different TIO₂, SIO₂, and AL₂O₃ proportions are conducted in a single-cylinder DI engine at a constant speed of 1500 rpm. The observations for fuel consumption, EGT, and emission parameters, such as CO, HC, NO_x, and smoke, are made. Based on the observations, BSFC and BTE are calculated, and the graphs are plotted for BSFC, BTE, CO, HC, NO_x, smoke, and EGT with engine brake power. A detailed result and discussion of individual parameters are given below.

5.1.1. Different Biodiesel with 20 and 100% Proportions. The 20 and 100% proportions of mamo additives are used in the experiments, and various parameters such as the time taken for fuel consumption, EGT, CO, HC, NO_x, and smoke are observed. The graphs are plotted for the variation of BSFC, BTE, EGT, emissions of carbon monoxide (CO), hydrocarbon (HC), oxides of nitrogen (NO_x), and smoke concerning brake power (BP).

5.1.1.1. Brake-Specific Fuel Consumption. The deviation of BSFC concerning BP for TIO2B40 and 100% proportions of 200 bar TIO2, and diesel is shown in Figure 8. It is seen that different proportions of biodiesel have higher BSFC than that diesel.

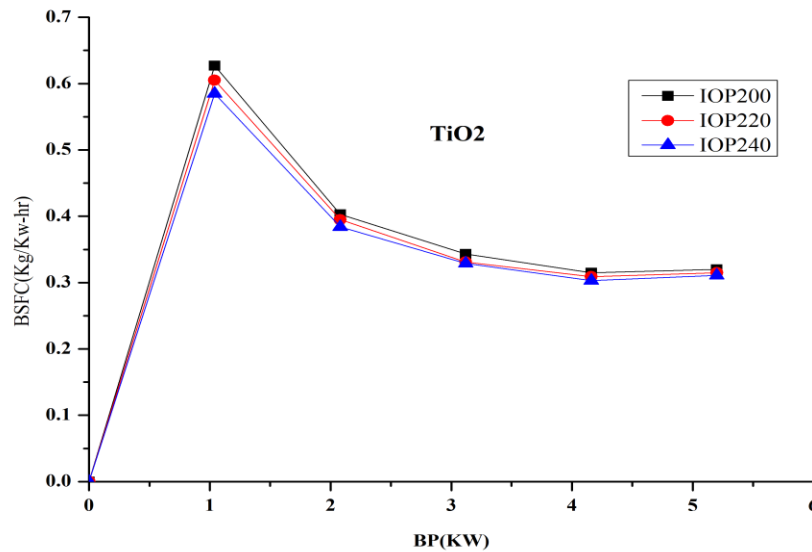


Figure 8: Deviation of BSFC vs BP for 20 and 100% blends of diesels.

It is due to the blends' high viscosity and poor volatility, which result in poor atomization and mixture formation. The BSFC for 100% biodiesel is higher compared to that of 20% proportion biodiesel. It is because 100% biodiesel has a lower heating value and requires excess fuel to maintain the same power output of the engine. Among the different proportions of diesel, TIO2B20 showed lower BSFC than other blends, which is very close to diesel fuel?

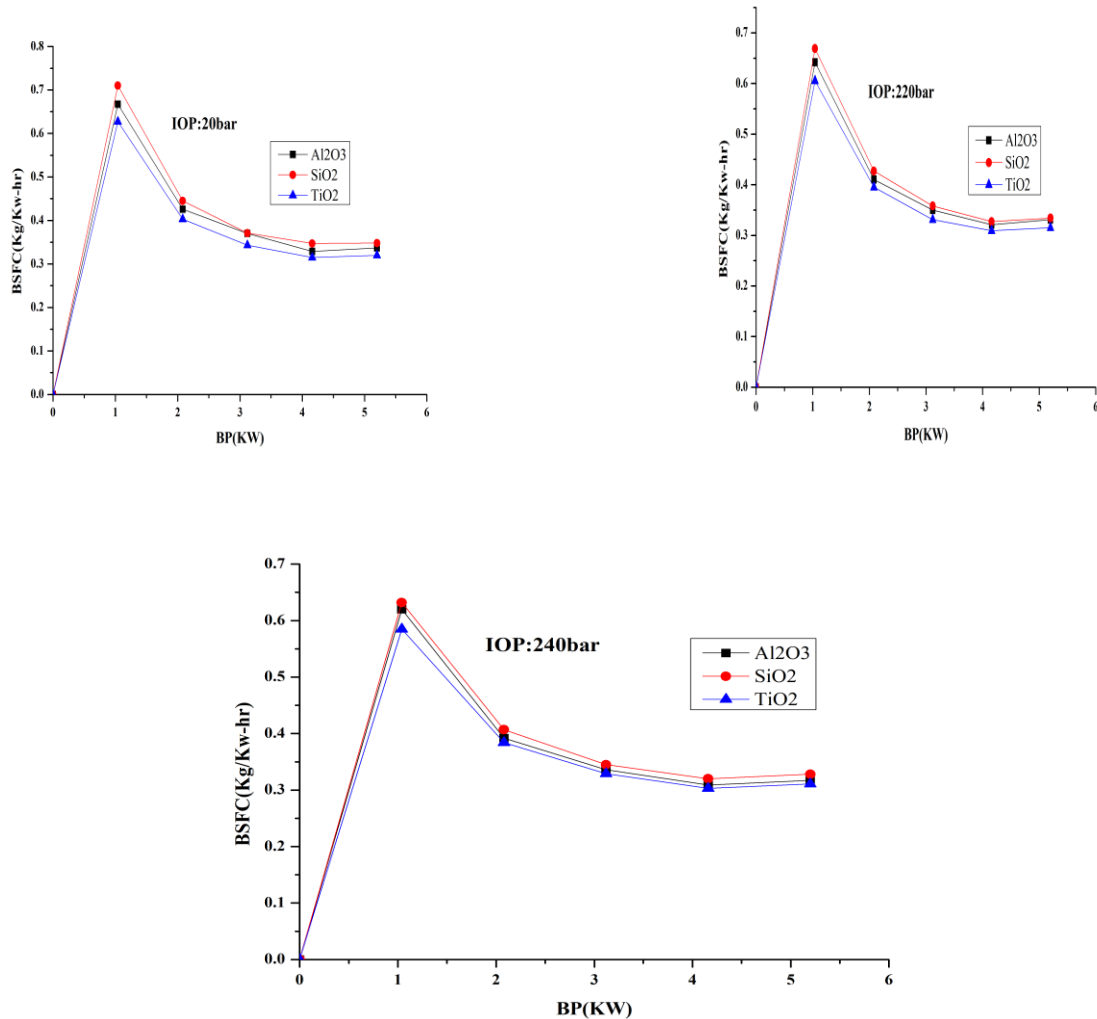


Figure 9: The Variation of BSFC with BP for various fuel blends

5.1.1.2. Brake Thermal Efficiency.

The deviation of BTE with respect to BP for 20 and 100% proportions of TIO₂, SIO₂, and AL₂O₃, and diesel is shown in Figure 9. It is evident from the graph that diesel showed higher BTE. This may be due to a higher calorific value and lower density of diesel.

Among the different proportions, B20 showed higher BTE but lower than diesel. It is mainly because of CV, cetane number, and density, which are almost equal to diesel fuel. It is also seen from the graph that 100% blends of three biodiesel indicated lower BTE than 20% blends. This may be due to the 20% blend having superior properties to 100% biodiesel.25 diesel.

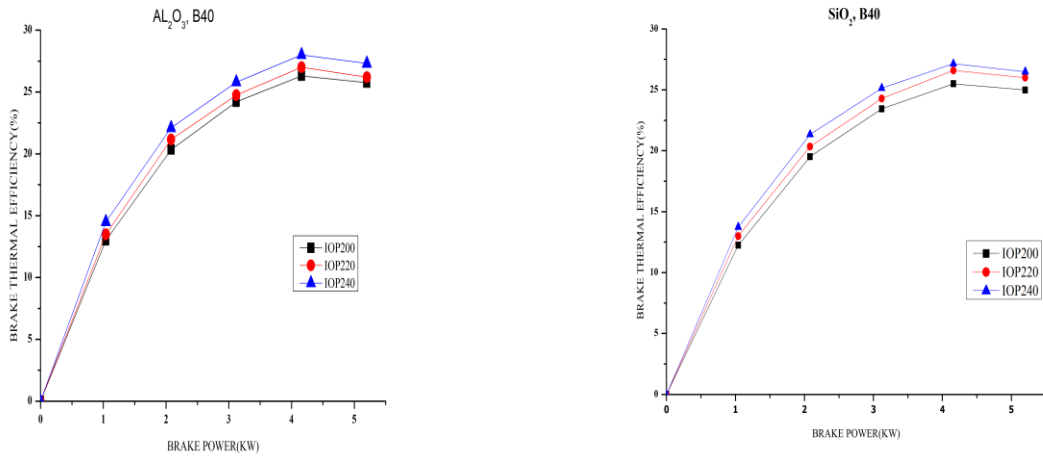
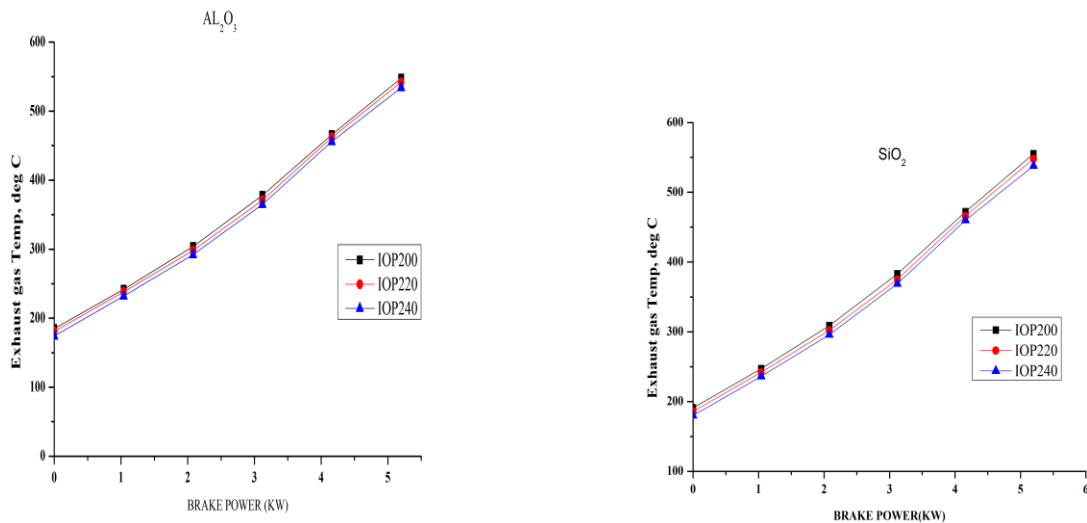


Figure 10: The variation of BTE with BP for various fuel blends

5.1.1.3. Exhaust Gas Temperature. The deviation of EGT concerning BP for 20 and 100% blends of TIO₂, AL₂O₃, and SIO₂, and diesel is shown in Figure 10. The EGT indicates



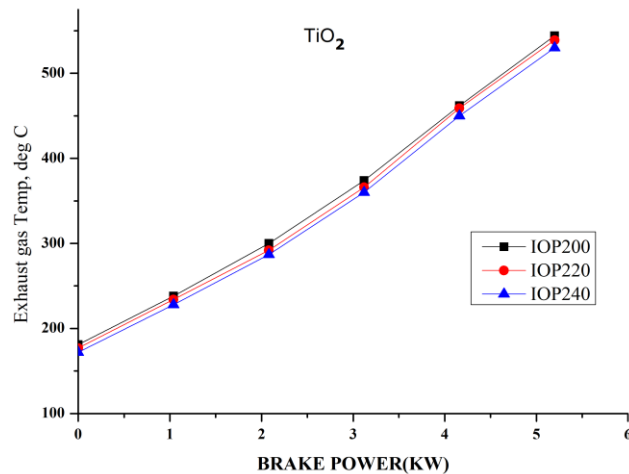


Figure 11: The variation of EGT with BP for various fuel blends

The heating capacity of the fuel used, and 1/3rd of the heat comes out as EGT. It is seen that EGT increases with the proportions of biodiesel at all loads. It is observed from the graph that B20 showed a higher EGT than others at all loads. Since B20 has a lower CV and higher density, incomplete combustion leads to an increase in EGT. It is also observed that B20 showed lower EGT among the blends and a slight increase compared to diesel. It is because B20 has excess oxygen, higher CV, and a lower density than other blends.

5.1.1.4. Carbon Monoxide Emission. The deviation of the CO concerning BP for 20 and 100% blends of TiO_2 , Al_2O_3 , and SiO_2 , and diesel is shown in Figure 11. It is seen from Figure 11 that MEMSO20 has lower CO emissions and diesel has higher emissions at all loads. This shows biodiesel contains more oxygen, leading to complete combustion. It indicates that the combustion efficiency improved, and the level of CO emission was reduced compared to diesel. The reason for the reduction of CO for B20 is the presence of excess oxygen and the effective combustion of biodiesel

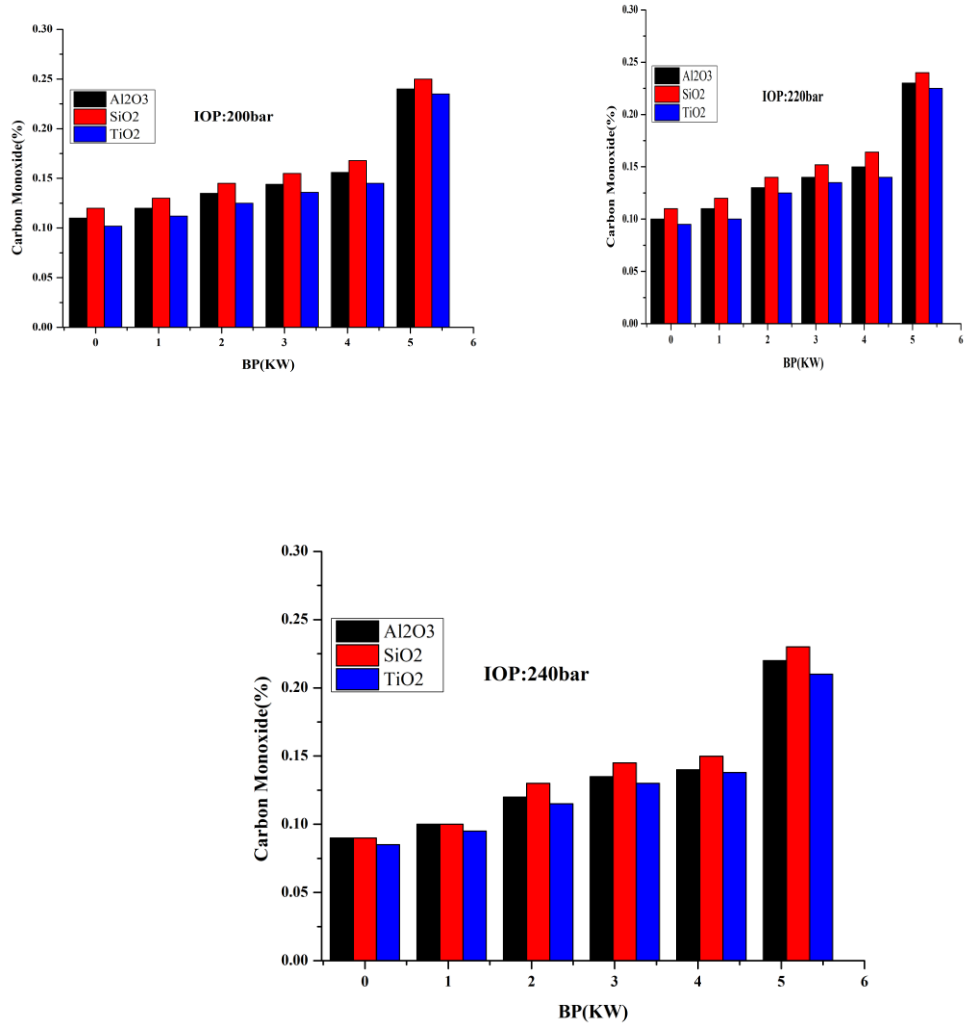


Figure 12: The variation of CO Emission with BP for various fuel blends

5.1.1.5. Hydrocarbon Emission. The deviation of HC concerning BP for 20 and 100% blends of TiO₂, Al₂O₃, and SiO₂ and diesel is shown in Figure 12. The HC emission for B20 is lower than that of other blend proportions and diesel at all load conditions.

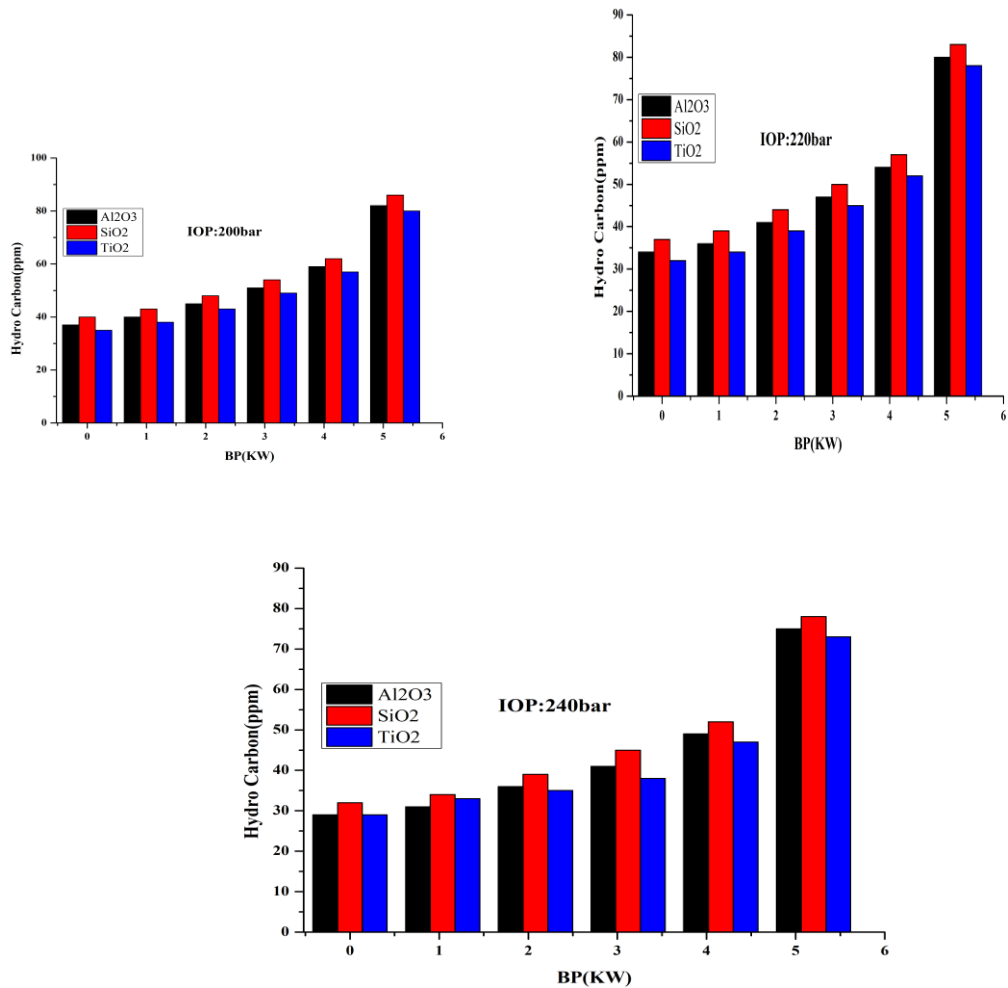


Figure 13: The variation of HC Emission with BP for various fuel blends

Since B20 has a higher heating value and leads to effective combustion. 24Among the different fuels, diesel showed higher HC emissions, which may be due to the diesel’s lack of oxygen, leading to poor atomization. It is seen that b40 shows higher HC emissions since it has a lower heating value than others.

5.1.1.6. Oxides of Nitrogen Emission.

The deviation of NO_x emission concerning BP for 20 and 100% blends of TIO₂, AL₂O₃, and SIO₂, and diesel is shown in Figure 13. The NO_x formation is based on the oxygen content of the fuel, combustion flame temperature, and reaction time in the combustion chamber. The NO_x emission of biodiesel blends is higher than that of diesel fuel and increases with load. It is due to the higher temperature of combustion and the presence of oxygen in the biodiesel, causing higher NO_x than that of diesel fuel. tio₂ has NO_x emissions lower than those of other blends among the different biodiesel blends.

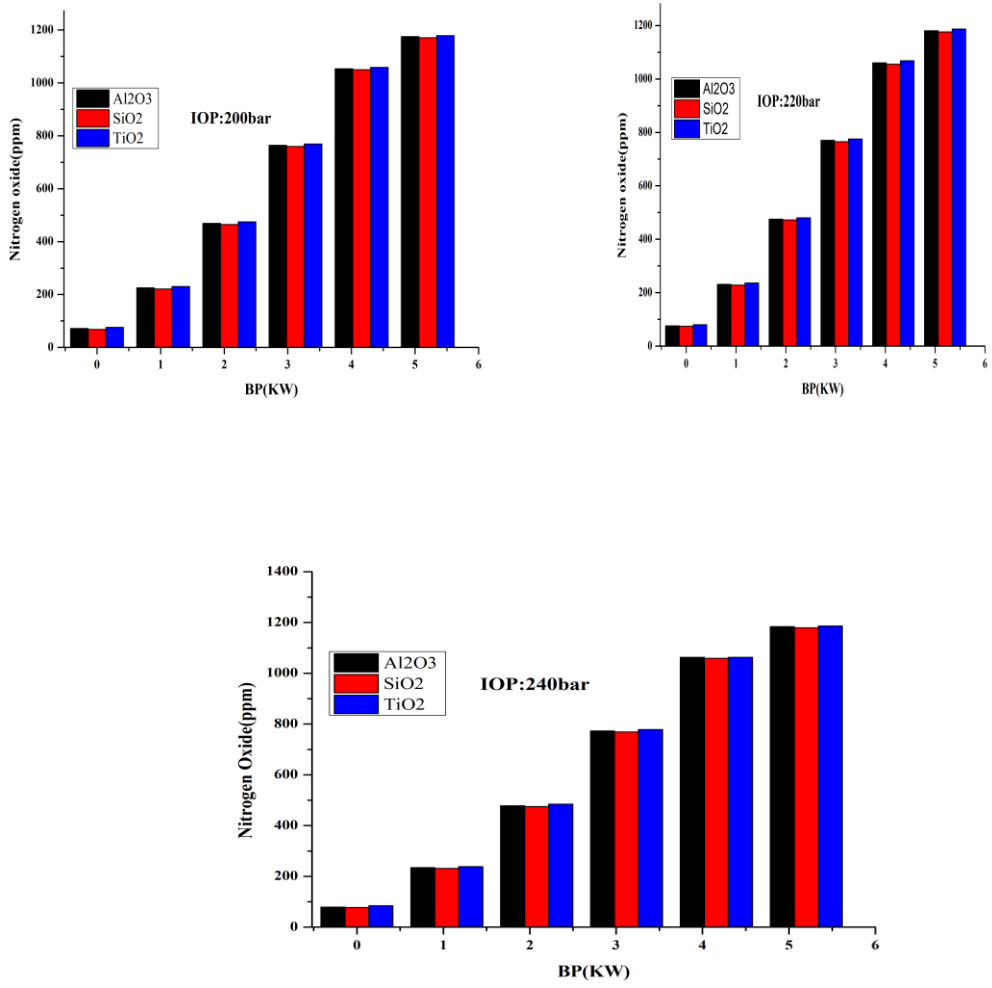


Figure 14: The variation of NOx with BP for various fuel blends

5.1.1.7. Smoke Opacity.

The deviation of smoke opacity emission concerning BP for 20 and 100% blends of TiO₂, Al₂O₃, and SiO₂ and diesel is shown in Figure 14. The smoke is produced more in the diffusive combustion phase.

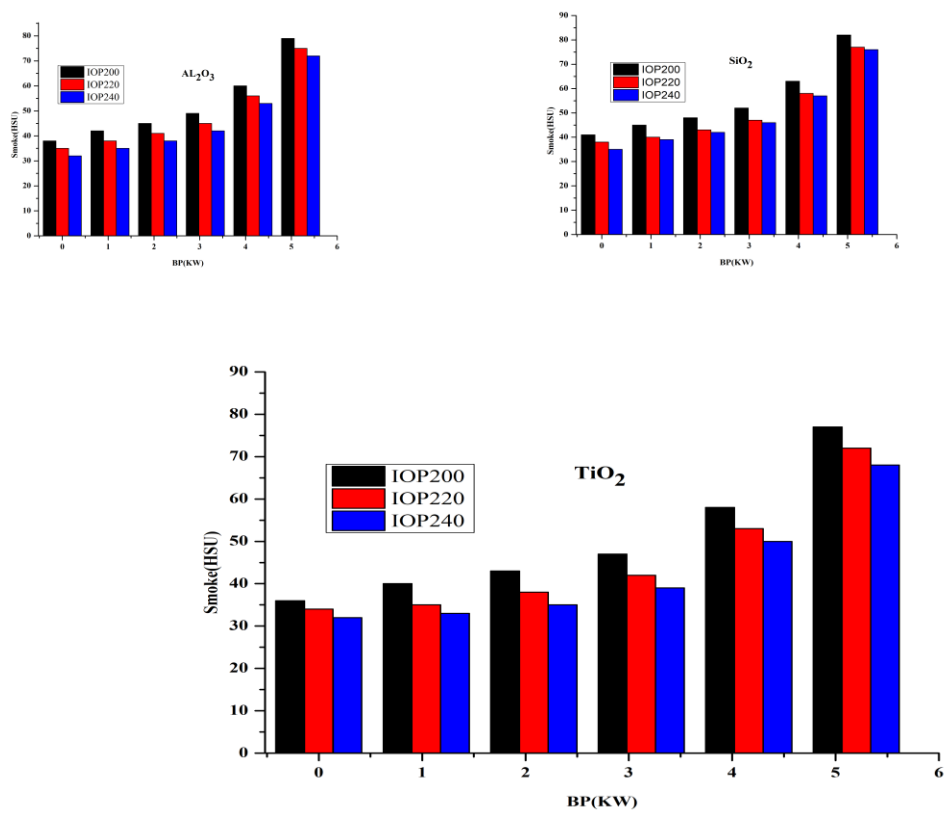


Figure 15: The variation of Smoke with BP for various fuel blend

Since oxygenated fuel blends such as TIO₂, AL₂O₃, and SIO₂ lead to an improvement in diffusive combustion. It is seen from the graph that the smoke opacity is lower for B40 at all loads. This is because of the higher heating value and excess oxygen in the fuel, which makes better combustion and reduces smoke opacity. 26 Among the biodiesel blends, B40 showed higher smoke opacity since it has a lower heating value and cetane number, which causes poor combustion and increases smoke opacity. Further, higher density at 100% blend leads to poor atomization. The diesel showed higher smoke opacity due to the presence of aromatic compounds compared to that of diesel

6. Conclusion

Different proportions of diesel blends and Pongamia oil with nano additives exhibit higher BSFC than diesel fuel due to high viscosity and volatility, resulting in poor atomization and mixture formation.

- 100% biodiesel blends demonstrate higher BSFC than 20% biodiesel blends due to their lower heating value, requiring excess fuel to maintain the same power output.
- Diesel fuel outperforms biodiesel blends in BTE in all load conditions due to its higher calorific value and lower density.
- Among the biodiesel blends, B20 exhibits higher BTE but still lower than diesel due to comparable properties like calorific value, cetane number, and density.
- EGT increases with the proportion of biodiesel blends in all loads. B40 has higher EGT due to its lower calorific value and higher density, resulting in incomplete combustion.
- B20 demonstrates lower EGT than other blends but slightly higher than diesel due to its excess oxygen content, higher calorific value, and lower density.
- Carbon monoxide (CO) emissions are lower in all biodiesel blends, particularly B20, than diesel in all load conditions, indicating complete combustion and improved efficiency.
- Hydrocarbon (HC) emissions are lower in MEMSO20 than in other blends and diesel fuel at all loads, while diesel exhibits higher HC emissions due to a lack of oxygen and poor atomization.
- Nitrogen oxide (NOx) emissions are higher in biodiesel blends than diesel fuel in all loads due to the higher combustion temperature and the presence of oxygen. AL2O3 demonstrates lower NOx emissions compared to other blends.
- Smoke opacity is lower in B20TIO2 at all loads than in other blends and diesel fuels due to a higher heating value and excess oxygen. B40TIO2 shows higher smoke opacity in comparison due to its lower heating value and cetane number. Diesel fuel has higher smoke opacity due to aromatic compounds.
- Adding an additive like such as TIO2, AL2O3, and SIO2 to diesel fuel does not significantly affect BTE. nano additives blends have higher BSFC than Biodiesel fuel due to a slight power loss. nano additives blend with 200 mg exhibits lower BSFC, suggesting more effective combustion.

Experimental findings indicate challenges with Biodiesel blends with higher BSFC and emissions, particularly NOx. Specific blend proportions, such as TIO2B40, show potential for improved performance and reduced emissions. Adding antioxidant additives such as LA may offer benefits such as improved fuel stability. Further research and optimization are required to enhance performance.

References

- 1) Ebrahimian, E.; Denayer, J. F. M.; Aghbashlo, M.; Tabatabaei, M.; Karimi, K. Biomethane and Biodiesel Production from Sunflower Crop: A Biorefinery Perspective. *Renewable Energy* 2022, 200, 1352– 1361.

- 2) Elgharbawy, A. S.; Ali, R. M. Techno-Economic Assessment of the Biodiesel Production Using Natural Minerals Rocks as a Heterogeneous Catalyst via Conventional and Ultrasonic Techniques. *Renewable Energy* 2022, 191, 161–175.
- 3) Mawlid, O. A.; Abdelhady, H. H.; El-Deab, M. S. Boosted Biodiesel Production from Waste Cooking Oil Using Novel SrO/ MgFe₂O₄ Magnetic Nanocatalyst at Low Temperature: Optimization Process. *Energy Convers. Manag.* 2022, 273, 116435.
- 4) Ashfaque Ahmed, S.; Soudagar, M. E. M.; Rahamathullah, I.; Sadhik Basha, J.; Yunus Khan, T. M.; Javed, S.; Elfasakhany, A.; Kalam, M. A. Investigation of Ternary Blends of Animal Fat Biodiesel- Diethyl Ether-Diesel Fuel on CMFIS-CI Engine Characteristics. *Fuel* 2023, 332, 126200.
- 5) Saravanan, A.; Karishma, S.; Senthil Kumar, P.; Jayasree, R. Process Optimization and Kinetic Studies for the Production of Biodiesel from Artocarpus Heterophyllus Oil Using Modified Mixed Quail Waste Catalyst. *Fuel* 2022, 330, 125644.
- 6) Yaashikaa, P. R.; Keerthana Devi, M.; Senthil Kumar, P.; Pandian, E. A review on biodiesel production by algal biomass: Outlook on lifecycle assessment and techno-economic analysis. *Fuel* 2022, 324, 124774.
- 7) Nayab, R.; Imran, M.; Ramzan, M.; Tariq, M.; Taj, M. B.; Akhtar, M. N.; Iqbal, H. M. N. Sustainable Biodiesel Production via Catalytic and Non-Catalytic Transesterification of Feedstock Materials - A Review. *Fuel* 2022, 328, 125254.
- 8) Wu, G.; Wang, X.; Abubakar, S.; Li, Y. A Skeletal Mechanism for Biodiesel-Dimethyl Ether Combustion in Engines. *Fuel* 2022, 325, 124834.
- 9) Rajendran, N.; Kang, D.; Han, J.; Gurunathan, B. Process Optimization, Economic and Environmental Analysis of Biodiesel Production from Food Waste Using a Citrus Fruit Peel Biochar Catalyst. *J. Clean. Prod.* 2022, 365, 132712.
- 10) Yahya, M.; Dutta, A.; Bouri, E.; Wadstrom, C.; Uddin, G. S. Dependence Structure between the International Crude Oil Market and the European Markets of Biodiesel and Rapeseed Oil. *Renewable Energy* 2022, 197, 594–605.
- 11) Zhu, X.; Liu, S.; Wang, Z.; Zhang, Q.; Liu, H. Study of the Effect of Methanol/Biodiesel Fuel Mixtures on the Generation of Soot Particles and Their Oxidation Reactivity. *Fuel* 2023, 341, 127632.
- 12) Maroušek, J.; Strunecký, O.; Bartoš, V.; Vochozka, M. Revisiting Competitiveness of Hydrogen and Algae Biodiesel. *Fuel* 2022, 328, 125317.
- 13) Szulczyk, K. R.; Badeeb, R. A. Nontraditional Sources for Biodiesel Production in Malaysia: The Economic Evaluation of Hemp, Jatropha, and Kenaf Biodiesel. *Renewable Energy* 2022, 192, 759–768.
- 14) Zhang, W.; Wang, C.; Luo, B.; He, P.; Zhang, L.; Wu, G. Efficient and Economic Transesterification of Waste Cooking Soybean Oil to Biodiesel Catalyzed by Outer Surface of ZSM-22 Supported Different Mo Catalyst. *Biomass Bioenergy* 2022, 167, 106646.
- 15) Iyyappan, J.; Jayamuthunagai, J.; Bharathiraja, B.; Saravananaraj, A.; Praveen Kumar, R.; Balraj, S. Production of Biodiesel from Caulerpa Racemosa Oil Using Recombinant Pichia Pastoris Whole Cell Biocatalyst with Double Displayed over Expression of Candida Antartica Lipase. *Bioresour. Technol.* 2022, 363, 127893.

- 16) (16) Zhang, X.; Li, N.; Wei, Z.; Dai, B.; Han, S. Synthesis and Evaluation of Bifunctional Polymeric Agent for Improving Cold Flow Properties and Oxidation Stability of Diesel-Biodiesel Blends. *Renewable Energy* 2022, 196, 737–748.
- 17) Sharma, P.; Sharma, A. K.; Balakrishnan, D.; Manivannan, A.; Chia, W. Y.; Awasthi, M. K.; Show, P. L. Model-Prediction and Optimization of the Performance of a Biodiesel - Producer Gas Powered Dual-Fuel Engine. *Fuel* 2023, 348, 128405.
- 18) Gohar Khan, S.; Hassan, M.; Anwar, M.; Zeshan; Masood Khan, U.; Zhao, C. Mussel Shell Based CaO Nano-Catalyst Doped with Praseodymium to Enhance Biodiesel Production from Castor Oil. *Fuel* 2022, 330, 125480.
- 19) Uyumaz, A. Experimental Evaluation of Linseed Oil Biodiesel/ Diesel Fuel Blends on Combustion, Performance and Emission Characteristics in a DI Diesel Engine. *Fuel* 2020, 267, 117150.
- 20) Yesilyurt, M. K. A Detailed Investigation on the Performance, Combustion, and Exhaust Emission Characteristics of a Diesel Engine Running on the Blend of Diesel Fuel, Biodiesel and 1-Heptanol (C7 Alcohol) as a next-Generation Higher Alcohol. *Fuel* 2020, 275, 117893.
- 21) Longati, A. A.; Campani, G.; Furlan, F. F.; Giordano, R. d. C.; Miranda, E. A. Microbial Oil and Biodiesel Production in an Integrated Sugarcane Biorefinery: Techno-Economic and Life Cycle Assessment. *J. Clean. Prod.* 2022, 379, 134487.
- 22) Sharma, V.; Kalam Hossain, A.; Ahmed, A.; Rezk, A. Study on Using Graphene and Graphite Nanoparticles as Fuel Additives in Waste Cooking Oil Biodiesel. *Fuel* 2022, 328, 125270.
- 23) Mahmoud, A. H.; Hussein, M. Y.; Ibrahim, H. M.; Hanafy, M.H.; Salah, S. M.; El-Bassiony, G. M.; Abdelfattah, E. A. Mixed Microalgae-Food Waste Cake for Feeding of *Hermetia Illucens* Larvae in Characterizing the Produced Biodiesel. *Biomass Bioenergy* 2022, 165, 106586.
- 24) Chen, Y.; Long, F.; Huang, Q.; Wang, K.; Jiang, J.; Chen, J.; Xu, J.; Nie, X. Biodiesel Production from *Rhodospiridium Toruloides* by Acidic Ionic Liquids Catalyzed Hydrothermal Liquefaction. *Bioresour. Technol.* 2022, 364, 128038.
- 25) Gupta, R.; McRoberts, R.; Yu, Z.; Smith, C.; Sloan, W.; You, S. Life Cycle Assessment of Biodiesel Production from Rapeseed Oil: Influence of Process Parameters and Scale. *Bioresour. Technol.* 2022, 360, 127532.
- 26) Wahyono, Y.; Hadiyanto, H.; Gheewala, S. H.; Budihardjo, M.A.; Adiansyah, J. S. Evaluating the Environmental Impacts of the Multi-Feedstock Biodiesel Production Process in Indonesia Using Life Cycle Assessment (LCA). *Energy Convers. Manag.* 2022, 266, 115832.
- 27) Manimaran, R.; Venkatesan, M.; Tharun Kumar, K. Optimization of Okra (*Abelmoschus Esculentus*) Biodiesel Production Using RSM Technique Coupled with GA: Addressing Its Performance and Emission Characteristics. *J. Clean. Prod.* 2022, 380, 134870.
- 28) Zhang, X.; Li, N.; Wei, Z.; Dai, B.; Lin, H.; Han, S. Enhanced the Effects on Improving the Cold Flow Properties and Oxidative Stability of Diesel-Biodiesel Blends by Grafting Antioxidant on PMAType Pour Point Depressant. *Fuel Process. Technol.* 2022, 238, 107483.